Parameters extraction of single diode model for degraded photovoltaic modules

M. Piliougine[a], R.A. Guejia-Burbano[a], G. Petrone[a], F.J. Sánchez-Pacheco[b], L. Mora-López[c], M. Sidrach-de-Cardona[d]

[a] *DIEM – University of Salerno. Via Giovanni Paolo II 132. 84084 Fisciano (SA), Italy*
[b] *Dpto. Tecnología Electrónica – University of Málaga. Málaga, Spain*
[c] *Dpto. Lenguajes y Ciencias de la Computación - University of Málaga. Málaga, Spain*
[d] *Dpto. Física Aplicada II - University of Málaga. Málaga, Spain*

Abstract

The single–diode model is widely used for the analysis of photovoltaic systems and reproducing accurately the *I–V* curve. Numerical or analytical methods can be employed to estimate the model parameters; among them explicit methods are well assessed providing precise results and low computational complexity, thus suitable to be developed on embedded systems. Due to their approximated nature, the accuracy of such methods may be affected by the operating conditions and by the state of health of the photovoltaic modules that have been characterised. The main contribution of this paper is to analyse a selection of explicit methods with the aim of testing their capability to detect degradation in photovoltaic modules. Since different degradation phenomena are reflected in a variation of the series resistance of the single diode equivalent circuit, the study is mainly focused on the estimation of this parameter. The comparison of different explicit methods has been done by using outdoor experimental *I–V* curves of a photovoltaic module operating in normal as well as degraded conditions. The analysis shows that only few methods exhibit enough reliability to estimate correctly the model parameters in presence of degradation and are less sensible to the environmental operating conditions.

Keywords: photovoltaic diagnosis, parameter identification, photovoltaic module simulation

1. Introduction

Photovoltaics (PV) is a key technology for the transition from the fossil fuel toward the decarbonized and sustainable energy supply [1]. Moreover, solar energy is available and abundant in a large part of the world and cannot be monopolised, thus the development of PV systems as well as other renewable sources is strategic for many countries. Research activities in the field of PV cell technology, power electronics, monitoring, controls and grid integration are mainly focused on improving the PV energy production and system reliability, thus increasing the overall efficiency of PV installations and reducing the cost. However, despite a very long lifetime (around 25 years) of PV modules, many studies [2] highlight that some degradation effects can be accelerated by various unpredictable and unavoidable phenomena which are related to the environmental and the operating conditions, the type of electrical connections and the manufacturing processes, among others [3].

Email addresses: mpiliouginerocha@unisa.it (M. Piliougine), rguejiaburbano@unisa.it (R.A. Guejia-Burbano), gpetrone@unisa.it (G. Petrone), fsanchezp@uma.es (F.J. Sánchez-Pacheco), llanos@uma.es (L. Mora-López), msidrach@uma.es (M. Sidrach-de-Cardona)

Some of these degradation mechanisms induce visible negative effects on the photovoltaic module, e.g discolouration of the encapsulation material, bubble formation or snail tracks, with possible detrimental effects on the photovoltaic electrical parameters [4]. Despite these visual defects, many faults and degradation phenomena cannot be distinguished with a visual inspection thus no information can be provided to users that could request the replacement of the modules if they do not meet the warranty, especially if the degradation is due to the manufacturing processes.

For these reasons, in the PV market there is an increasing interest into non–invasive and cheap functionalities to be integrated into PV plants in order to identify early degradation of PV panels. On–site monitoring systems are aimed to provide/report information about the energy production, operating conditions and analysis of different faults. In this scenario, diagnostic functions allow to detect quickly the faulty PV modules and to estimate the difference between the produced energy and the expected one, thus supporting the owners of PV plants to reduce the payback time and maximise the profit from the produced energy. In [5] a review of effective, low cost, and viable PV monitoring systems for small and medium scale PV plants is shown.

As described in literature [6], the diagnostic procedures could be classified into *"off–line"* and *"on–line"* methods. The *"off–line"* methods require to disconnect the module from the photovoltaic array to be measured and characterised independently. On the contrary, *"on–line"* methods use information acquired while the module is working without disconnecting it from the array. Due to their low cost and flexible configurations, embedded systems installed on site are used to perform the measurement and process the experimental data. As *"on-line"* diagnostic methods are directly implemented on this type of devices, it is useful that the equations required to implement those methods are as simple as possible to speed up the data processing, avoiding implicit expressions and iterative procedures.

In the literature it is possible to find two different approaches to characterise a photovoltaic panel (and hence having a tool to estimate the degradation). The first type relies on the performing of a comparison between the solar energy received by the PV module, and the electrical energy delivered through its terminals and estimated by means of its electrical measurement [7–9]. The electrical behaviour of a photovoltaic module under specific conditions of irradiance and cell temperature is described in terms of its I-V curve [10]. In order to estimate the energy input it is required a solar irradiance sensor and a cell temperature sensor attached to the module, then the PV performance, in a given window of time, is obtained by calculating an indicator denominated Performance Ratio [11]. The evolution of this performance indicator throughout time allows to detect the possible degradation in terms of energy production [12]. The drawback of this approach is that hardly the required sensors are available due to their high costs [13], and in the case of having them, there are multiple associated problems related to the inaccuracy of measurement and their periodically calibration and cleaning [14].

Other techniques, usually defined as *"model–based"* approaches, consist on the identification of some parameters associated to models that are suitable to describe accurately the electrical behaviour of the photovoltaic devices. Depending on the evolution of these parameters, the degradation could be diagnosed and estimated [15, 16]. The identification of the values of these parameters could be done from the data obtained only from its I-V curve without measuring the irradiance. Moreover, some of these methods only require a few selected points of the I-V curve.

The most popular photovoltaic electrical models are the Single Diode Model (SDM) and the Double Diode Model (DDM) [17], both derived from Schottky diode equation with the addition of a series resistance and a parallel resistance for taking into account the losses inside the PV device. For both models the relationship between voltage and current (mathematical model of the PV module) is described by a non–linear and implicit equation with five unknown parameters for the SDM and seven unknown parameters for the DDM.

In the literature, it is possible to find a lot of different methods to determine a valid set of the parameters values [18–21]. However, there are also works that are only able to estimate a reduced subset of the parameters [22–24], even some that are only focused on the identification of the series and shunt resistances [25, 26], since internal resistances are indicators of some degradation phenomena. For example, the series resistance is affected by corrosion in the electrical contacts, soldering problems and degradation of the cells, among others [27].

Since this work focuses on the *on–line* estimation of these parameters, it is preferred to avoid the execution of iterative procedures to reduce the computational burden. As it is shown in [28] or in [29], many papers propose simple procedures or explicit equations for calculating the parameters of the SDM model [30–38]. Such approaches are potentially suitable to be easily integrated in the *on–line* diagnostic function. Nevertheless, such papers test the methods by using data coming from the specifications or by using experimental I–V curves acquired in normal operating conditions thus by validating the identification methods only in non–degraded conditions.

The main contribution of this paper is aimed at investigating the reliability of the aforementioned explicit methods, also said *direct methods*, to identify the parameters of the photovoltaic panel that are indicators of possible degradation phenomena, in particular the internal series and parallel resistances. In other words, the goal is to study the reliability of such methods when they are used for diagnostic purposes.

In this work, among all the explicit approaches for parameter identification of the SDM model, four explicit methods have been selected to be compared and analysed (all of them based on a reduced set of simple and direct formulas). By referring to the classification given in [28], among the most promising ones, two methods have been selected among the ones that use only information as given in the PV panel data sheet, and two methods based on the slopes calculated in the short–circuit current and open–circuit voltage.

In order to have a reference value as accurate as possible for the identified parameters, a non–explicit method based on an iterative fitting procedure has been also applied. All these methods will be tested by using measurements from several experiments in which different levels of degradation are emulated by connecting in series with the photovoltaic module external resistances with different nominal values. The objective is to study the capability of the methods to detect this simulated degradation effect added to the PV module that is operating for several days under outdoor conditions.

The paper is organised as follows: Section 2 describes briefly the SDM and the different methods used in this paper for identifying the five parameters of this model. Section 3 starts referring to the experimental system used for acquiring the outdoor I–V curves of the photovoltaic module under study. In addition, the procedure to select I–V curves and estimation of the main electrical parameters are explained. The section ends describing how further degradation has been emulated by connecting additional resistances in series. Section 4 is aimed at showing and comparing the results obtained by the different methods in the nominal operating conditions by using the numerical curve-fitting approach as the reference. The capability of these approaches

for reconstructing the measured I–V curve is also analysed. In Section 5, the behaviour of the identification methods with I–V curves measured in degraded condition is studied. Finally, in Section 6, the main conclusions of this work are summarised.

2. Photovoltaic model and parameter identification methods

2.1. Single Diode Model

Figure 1 shows the SDM equivalent electrical circuit of a PV device [17]. It can be scaled–up or down to be adapted to a single PV cell, a PV module or a PV array, depending on the number of cells connected in series and parallel (N_s and N_p respectively). The corresponding SDM equation for a photovoltaic module is given in (eq 1).

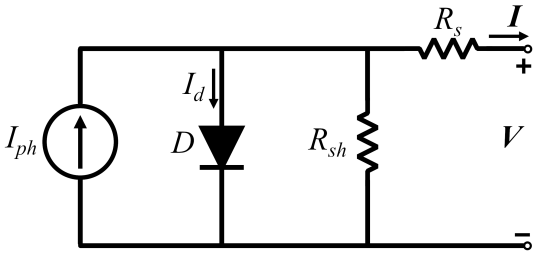

Figure 1: Equivalent circuit of the single diode model

$$I = I_{ph} - I_0 \cdot \left(exp\left\{ \frac{V + I \cdot R_s}{N_s \cdot n \cdot V_t} \right\} - 1 \right) - \frac{V + I \cdot R_s}{R_{sh}} \tag{1}$$

where V is the voltage between the terminals of the photovoltaic module (V), I is the output current (A), I_{ph} is the photo-generated current (A), I_0 is the dark saturation current (A), n is the diode ideality factor (dimensionless), R_s is the series resistance (Ω), R_{sh} is the shunt or parallel resistance (Ω) and N_s is the number of cells in series.

In addition, V_t is the thermal voltage (V) given by kT/e, being k the Boltzmann constant ($1.380\,649 \times 10^{-23}$ JK^{-1}), e the elementary electric charge ($1.602\,176\,634 \times 10^{-19}$ C) [39] and T the cell temperature expressed in kelvin (with $T = 273.15 + T_m$ if T_m is expressed in °C).

To reproduce accurately the I–V curve of a PV array, it is not enough to have a good mathematical model (e.g. the SDM), but it is also necessary to correctly determine or estimate its parameters. The lasts can vary from one cell/module to another and depend on the operating conditions, thus resulting extracted parameters influence the final accuracy of the adopted model [40]. There are many deterministic and stochastic procedures available to calculate the free five parameters (I_{ph}, I_0, n, R_s and R_{sh}). A previous paper [41] provides an extensive review of works related to the modelling and parameter estimation of photovoltaic (PV) cells, mainly devoted to the PV simulation. Among them, the explicit methods are strongly appreciated due to the fact that they provide acceptable results with very few computational burden [42]. They usually exploit the three notable points that an I-V curve passes through: the short–circuit current I_{SC} , the open–circuit voltage V_{OC} and the maximum power point (V_{Pmax}, I_{Pmax}). In some cases, the slopes of the I–V curve calculated in I_{SC} and V_{OC} are also needed.

In this work four explicit methods have been selected among the most promising ones analysed in [28] and briefly recalled in the subsections 2.2–2.5. Since there is no way to perform a direct measurement of the five parameters of the SDM model, in order to have a reference value for each parameter, a non–explicit method has been used to have a reference value for each parameter. Following the classification proposed by [28], the selected approach lies within the *"optimisation methods"*, because it uses all the measured points of the I–V curve in order to construct an error function to be minimised by means of an iterative procedure. This method is described in section 2.6.

2.2. Explicit equations based on the LambertW function

This method exploits the Lambert W–function [43] for deriving the set of explicit equations allowing a fast calculation of the SDM parameters. In [17, 42, 44] all details about this approach are provided:

$$I_{ph} \simeq I_{\mathrm{SC}} \tag{2}$$

$$E_g(T) = E_{g0} - \frac{a \cdot T^2}{T + b} \tag{3}$$

$$I_0 = I_{\mathrm{SC}} \cdot \exp\left\{ \left(\frac{V_{\mathrm{OC}}}{V_{\mathrm{OC}} - \beta \cdot T} \right) \cdot \left(\frac{\alpha \cdot T}{I_{\mathrm{SC}}} - 3 - \frac{E_g(T)}{V_t} \right) \right\} \tag{4}$$

$$A = \frac{V_{\mathrm{OC}}}{\ln\left(\frac{I_{\mathrm{SC}}}{I_0} + 1 \right)} \qquad B = \frac{V_{\mathrm{Pmax}} \cdot (V_{\mathrm{Pmax}} - 2 \cdot A)}{A^2} \tag{5}$$

$$n = \frac{A}{N_s \cdot V_t} \tag{6}$$

$$C = \frac{V_{\mathrm{Pmax}} \cdot (2 \cdot I_{\mathrm{Pmax}} - I_{ph})}{A \cdot I_0} \quad x = W_0\{ C \cdot \exp(B) \} - B \tag{7}$$

$$R_s = \frac{x \cdot A - V_{\mathrm{Pmax}}}{I_{\mathrm{Pmax}}} \tag{8}$$

$$R_{sh} = \frac{x \cdot A}{I_{ph} - I_{\mathrm{Pmax}} - I_0 \cdot (\exp(x) - 1)} \tag{9}$$

where α is the current–temperature coefficient of the module expressed in AK^{-1}, β is the voltage–temperature coefficient in VK^{-1} and $W_0\{\cdot\}$ is the main branch of the Lambert$-W$ function. Finally $E_g(T)$ is the band gap energy (eV) of the semiconductor at temperature T (K); the constants E_{g0} (band gap energy at 0 K), a and b depend on the material. In the case of single–crystalline silicon (sc-Si) the values are $E_{g0} = 1.16$ eV, $a = 7 \times 10^{-4}$ eV K^{-1} and $b = 1100$ K [45]. This approach will be identified in the following as ***LambertW method***.

2.3. Explicit equations by using the Serial–Parallel Ratio

In [35, 36] it has been shown that the 5–parameter SDM can be scaled down to 4–parameter SDM without losing significant precision if only one resistance is neglected. The method allows to classify the PV modules into two groups on the basis of the value assumed by the performance indicator named Serial–Parallel–Ratio (*SPR*):

$$I_{ph} \simeq I_{\mathrm{SC}} \qquad \gamma_i = \frac{I_{\mathrm{Pmax}}}{I_{\mathrm{SC}}} \qquad \gamma_v = \frac{V_{\mathrm{Pmax}}}{V_{\mathrm{OC}}} \tag{10}$$

$$r = \frac{\gamma_i \cdot (1-\gamma_v)}{\gamma_v \cdot (1-\gamma_i)} \qquad SPR = (1-\gamma_i) \cdot \exp(r) \tag{11}$$

$$\text{Case (A)}: \; SPR > 1 \Rightarrow \begin{cases} R_{sh} = \infty \\ \delta = \ln(1-\gamma_i) \\ R_s = \dfrac{V_{\mathrm{OC}}}{I_{\mathrm{SC}}} \cdot \dfrac{\dfrac{\gamma_v}{\gamma_i} \cdot (1-\gamma_i) \cdot \delta + (1-\gamma_v)}{(1-\gamma_i) \cdot \delta + \gamma_i} \\ A = \dfrac{I_{\mathrm{Pmax}} \cdot R_s - V_{\mathrm{OC}} + V_{\mathrm{Pmax}}}{\delta} \\ I_0 = I_{ph} \cdot \exp\left(\dfrac{-V_{\mathrm{OC}}}{A}\right) \end{cases} \tag{12}$$

$$\text{Case (B)}: \; SPR < 1 \Rightarrow \begin{cases} R_s = 0\,\Omega \\ \lambda_1 = \dfrac{(1-\gamma_v) \cdot (2 \cdot \gamma_i - 1)}{(1-\gamma_i) \cdot (\gamma_i + \gamma_v - 1)} \\ \lambda_2 = \dfrac{\gamma_v}{1-\gamma_i} \\ \omega = W_{\text{-}1}\{ - SPR \cdot \lambda_1 \cdot \exp(-\lambda_1)\} \\ R_{sh} = \dfrac{V_{\mathrm{OC}}}{I_{\mathrm{SC}}} \cdot \dfrac{\lambda_2 \cdot \omega + \lambda_1}{\omega + \lambda_1} \\ A = \dfrac{-V_{\mathrm{OC}} + V_{\mathrm{Pmax}}}{\ln\left\{\dfrac{(I_{\mathrm{SC}} - I_{\mathrm{Pmax}}) \cdot R_{sh} - V_{\mathrm{Pmax}}}{I_{\mathrm{SC}} \cdot R_{sh} - V_{\mathrm{OC}}}\right\}} \\ I_0 = \left(I_{ph} - \dfrac{V_{\mathrm{OC}}}{R_{sh}}\right) \cdot \exp\left(\dfrac{-V_{\mathrm{OC}}}{A}\right) \end{cases} \tag{13}$$

where $W_{\text{-}1}\{\cdot\}$ is the lower branch of the Lambert$-W$ function and n could be calculated as in the previous methods using (eq 6). This approach will be identified in the following as ***SPRatio method***.

2.4. Explicit equations based on the Phang's method

The method proposed in [30] uses the values of the slopes at the short–circuit and open–circuit points (R_{sh0} and R_{s0} respectively) as starting points. The regression procedures to estimate these values can be performed over the set $\{V_i, I_i\}$ or over $\{I_i, V_i\}$:

$$R_{s0} = -\left.\frac{dV}{dI}\right|_{I=0} = -\frac{1}{\left.\dfrac{dI}{dV}\right|_{V=V_{\mathrm{OC}}}} \tag{14}$$

$$R_{sh} = R_{sh0} = -\left.\frac{dV}{dI}\right|_{I=I_{\mathrm{SC}}} = -\frac{1}{\left.\frac{dI}{dV}\right|_{V=0}} \tag{15}$$

$$B = I_{\mathrm{SC}} - \frac{V_{\mathrm{Pmax}}}{R_{sh}} - I_{\mathrm{Pmax}} \qquad C = I_{\mathrm{SC}} - \frac{V_{\mathrm{OC}}}{R_{sh}} \tag{16}$$

$$A = \frac{V_{\mathrm{Pmax}} + R_{s0} \cdot I_{\mathrm{Pmax}} - V_{\mathrm{OC}}}{\ln(B) - \ln(C) + \frac{I_{\mathrm{Pmax}}}{C}} \tag{17}$$

$$D = \exp\left(-\frac{V_{\mathrm{OC}}}{A}\right) \qquad I_0 = C \cdot D \qquad R_s = R_{s0} - \frac{A}{I_0} \cdot D \tag{18}$$

$$I_{ph} = I_{\mathrm{SC}} \cdot \left(1 + \frac{R_s}{R_{sh}}\right) + I_0 \cdot \left[\exp\left(\frac{I_{\mathrm{SC}} \cdot R_s}{A}\right) - 1\right] \tag{19}$$

Finally, for the estimation of the diode ideality factor n it is possible to use (eq 6). This set of equations will be noted as ***Phang method***.

2.5. Explicit equations based on the Toledo's method

The method proposed in [34] rewrites the SDM equation given in (eq 1) differently. In this case, the general equation for the SDM is expressed as:

$$I = A - B \cdot (C^V \cdot D^I - 1) - E \cdot V \tag{20}$$

The method needs the set of values at the short–circuit point and three additional points of the *I-V* curve $\{(V_1, I_1), (V_2, I_2), (V_3, I_3)\}$. These values are the starting points for calculating the model of five parameters. Although the choice of these points could be arbitrary, the author suggests choosing three set of points with voltage greater than the maximum power-point and uniformly distributed. In this paper, these additional three points are the maximum power point, the open-circuit point and the maximum of the $\alpha-$power function [20], that taking ($\alpha = 10$) is a point between V_{Pmax} and V_{OC}. The proposed set of equations is:

$$E = -\left.\frac{dI}{dV}\right|_{V=0} = -\frac{1}{\left.\frac{dV}{dI}\right|_{I=I_{\mathrm{SC}}}} \tag{21}$$

$$F_1 = \ln(I_{\mathrm{SC}} - E \cdot V_1 - I_1) \tag{22}$$

$$F_2 = \ln(I_{\mathrm{SC}} - E \cdot V_2 - I_2) \tag{23}$$

$$F_3 = \ln(I_{\mathrm{SC}} - E \cdot V_3 - I_3) \tag{24}$$

$$D = \exp\left\{\frac{(F_1 - F_2) \cdot (V_2 - V_3) - (F_2 - F_3) \cdot (V_1 - V_2)}{(I_1 - I_2) \cdot (V_2 - V_3) - (I_2 - I_3) \cdot (V_1 - V_2)}\right\} \tag{25}$$

Table 1: Interval and start points for the five SDM parameters

	Lower limit	Upper limit	Start point
$I_{ph}[A]$	1/12	12	I_{SC}
$I_0[nA]$	1×10^{-3}	1×10^{4}	5×10^{3}
$n[/]$	1	2	1.5
$R_s[\Omega]$	0	100	$-dV/dI\ at\ V = V_{\mathrm{OC}}$
$R_{sh}[\Omega]$	1	5×10^{4}	$-dV/dI\ at\ I = I_{\mathrm{SC}}$

$$C = \exp\left\{\frac{F_2 - F_3 - (I_2 - I_3)\cdot\ln(D)}{V_2 - V_3}\right\} \tag{26}$$

$$B = \exp\left\{F_1 - V_1\cdot\ln(C) - I_1\cdot\ln(D)\right\} \tag{27}$$

$$A = I_{\mathrm{SC}} - B \tag{28}$$

$$G = \frac{\ln(C)}{\ln(C) - E\cdot\ln(D)} \tag{29}$$

$$I_{ph} = A\cdot G \qquad I_0 = B\cdot G \tag{30}$$

$$R_s = \frac{\ln(D)}{\ln(C)} \qquad R_{sh} = \left(\frac{1}{E} - R_s\right) \tag{31}$$

$$n = \frac{1}{N_s\cdot V_t\cdot\ln(C)} \tag{32}$$

2.6. Identification method based on curve fitting

The algorithm used to find the optimal values of the SDM parameters is widely known as trust–region–reflective. A comprehensive guide about this family of techniques can be found in [46].

There is a specific type of trust–region algorithm able to work when the search space is bound to a feasible region. This means that users can define an interval for each parameter to estimate in addition to the required initial point. Fixing an appropriate set of lower and upper limits is not an easy task but it is possible to find some proposals in the literature that are suitable for the SDM [47, 48]. Specifically, the second of those works defines a feasible region taking into account the information from a large database of photovoltaic modules and their features. Table 1 presents the values of these intervals, that have been also used in this paper. In addition, the table provides the start point that has been selected for each parameter. The initial values for R_s and R_{sh} are the slopes of the *I-V* curve in V_{OC} and I_{SC} respectively, for I_{ph} the initial point is I_{SC} due to their high correlation. For n and I_0, without any additional information, the centres of the proposed intervals have been adopted as the starting points.

The trust–region algorithm integrated into the Optimisation Toolbox of Matlab [49] has been used in this paper. In the call to this function it is necessary to pass some important tuning parameters in order to ensure

Table 2: Tuning parameters for the fitting procedure

	Default value	Used value
maxIter	400	2500
maxFunEvals	600	10000
tolX	1×10^{-6}	1×10^{-12}
tolFun	1×10^{-6}	1×10^{-12}

a successful execution. Among these input values, the maximum number of iterations (*maxIter*), the minimum tolerance in the search space (*tolX*) and the minimum tolerance in the target function (*tolFun*) have been setled. When any of these criteria is reached, the function stops its execution. It is worth to note that, due to the strong non-linearity of the SDM model, if the Matlab function uses default setting the convergence to the optimal solution is not assured. Table 2 shows the difference between the default values and the ones used in this paper.

The numerical solving procedure provides not only an estimation for each parameter of the SDM model, but also a confidence interval around that value. In this paper the confidence interval is referring to a confidence level of 99%, which means that with a probability of 0.99 the true value of the parameter is inside that interval. Error bars will be always attached to the plots referring to this method in order to visualise this confidence interval.

This approach will be identified in the following as ***Fitting method***.

3. Experimental methodology

3.1. Measurement system and setup

In order to analyse and compare the explicit methods for SDM parameter identification, a PV measurement system has been configured for acquiring a large number of *I–V* curves under outdoor conditions. The equipment is installed on the roof of the *Department of Applied Physic II* at the University of Málaga (latitude: 36.715° N ; longitude: 4.478° W; elevation: 60 m). The PV module under test is the model *I–53* from the manufacturer *Isofotón* and its data-sheet specifications are summarised in Table 3. In [50] there is a detailed description of the measurement system used and a deep analysis of uncertainties. This equipment is able to acquire simultaneously the *I–V* curves and other external variables such as the in-plane irradiance G_{I} (solar power per square metre incident on the module plane) and the temperature of the module. The system is controlled by a software running in a personal computer in order to take automatic measurements every three minutes from the sunrise to the sunset. This software stores the measurements in a relational database and the data is available to be downloaded throughout a web page accessible from any computer in Internet. A full description of this application can be found in [51].

A first analysis has been done for calculating the actual SDM parameters to be assumed the baseline for estimating the capability of explicit methods to evaluate correctly additional degradation induced artificially. Indeed, to simulate further levels of degradation in the real PV system, some resistors with different nominal

Table 3: Isofotón I-53 main specifications

Parameter	Symbol	Value
Maximum Output Power at STC (W)	$P_{\text{max STC}}$	53
Voltage at Maximum Power (V)	$V_{\text{Pmax STC}}$	17.4
Current at Maximum Power (A)	$I_{\text{Pmax STC}}$	3.05
Short Circuit Current at STC (A)	$I_{\text{SC STC}}$	3.27
Open Circuit Voltage at STC (V)	$V_{\text{OC STC}}$	21.6
$I_{\text{SC STC}}$ temperature coefficient (AK^{-1})	α	0.001326
$V_{\text{OC STC}}$ temperature coefficient. (VK^{-1})	β	-0.07704
Series resistance (new module) (Ω)	R_s	0.288
Number of Cells in series	N_s	36
Cell Type	$sc-Si$	mono
Cell Area (cm^2)	A_c	104.4

values are connected in series to the PV module terminals. Figure 2 shows the electrical connections of the external resistors and measurement points.

The system has been programmed to perform several days of measurements for each different configuration, in order to ensure a perfect clear sky day for each of the experiments: 0 Ω (no additional series resistor), 0.3 Ω, 1 Ω and 1.5 Ω. The highest values of the additional series resistor have been selected according to the analysis given in [52] where it has been shown that R_s reaches values up to 2.3 Ω over an operation period of 20 year. The experiments have been performed during a period of time between June and July 2018.

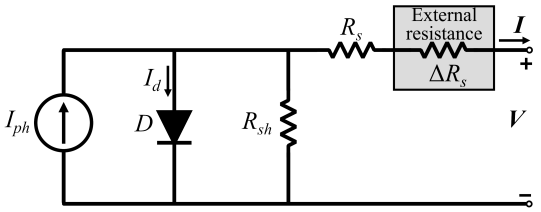

Figure 2: SDM with additional series resistance

3.2. Data pre–processing

As a result of the four performed experiments, there are available hundreds of I–V curves at different levels of irradiance and module temperature conditions, as well as with different additional series resistances.

Once all the experiments have been finished all the I–V curves have been downloaded from the server and the files have been imported in Matlab workspace format for their further processing.

The first step is to remove all the measurements that do not satisfy the following criteria:

- The irradiance is measured before and after the measurement of each I–V curve. If the difference between both readings is greater than 5 Wm^{-2} the curve is rejected.

- All the measurements done with an irradiance lower than 700 Wm^{-2} have been removed because the single diode model is more accurate for high irradiance levels [53].

- In order to be sure that all the I–V curves have a suitable shape, a visual inspection of all selected curves has be done by using a plotting function in Matlab. If it is noticed that a particular curve presents a weird shape (due to a shadow or a measurement error), it is eliminated from the dataset.

The second step is the calculation of the notable points $(0,\ I_{\mathrm{SC}})$, $(V_{\mathrm{OC}},\ 0)$ and $(V_{\mathrm{Pmax}},\ I_{\mathrm{Pmax}})$ from the experimental I–V curves in addition to the slopes of the curves in I_{SC} and V_{OC}.

It is worth to note that the accurate calculation of such values from the experimental data is crucial for not introducing additional errors in the SDM parameter estimation, since the identification of SDM parameters by means of explicit methods is strongly dependent on I–V notable points and slopes.

The typical experimental I–V curve is given by a sequence of discrete current-voltage pairs starting in some point close to I_{SC} and finishing in another point close to V_{OC}. However, neither I_{SC} nor V_{OC} values might be included in the set of measured points and both need to be estimated by linear interpolation. Even worse for $(V_{\mathrm{Pmax}},\ I_{\mathrm{Pmax}})$ point, that should be detected by using a non–linear interpolation. For each I–V curve, the technique described in [54] is used to calculate notable points and slopes.

The measured point nearest to the $Y-axis$ is identified being its current value I_x and from the nearest one to the $X-axis$ we get also its voltage component V_y. Then a two–dimensional interval centred in I_x is made $[0,\ 20\%\cdot V_y]\times[I_x-4\%\cdot I_x,\ I_x+4\%\cdot I_x]$. The interpolation with all the points inside the interval allows us to determine I_{SC} and also the slope (dI/dV) when $I=I_{\mathrm{SC}}$. Analogous, using linear interpolation again over the interval $[V_y-10\%\cdot V_y,\ V_y+10\%\cdot V_y]\times[-20\%\cdot I_x,\ 20\%\cdot I_x]$ the value of V_{OC} and the slope (dI/dV) when $V=V_{\mathrm{OC}}$ are determined. Figure 3 and (eq 33) show the concept of the slopes and their relationship with the I–V curve. The values of I_{SC} and V_{OC} represent the cuts for the Y and X axes.

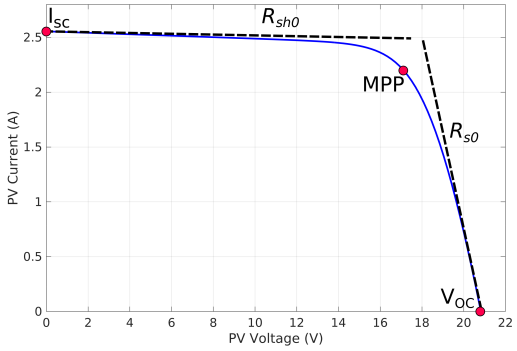

Figure 3: Slopes approximation on the I–V curve

$$R_{sh0}=-\left.\frac{dV}{dI}\right|_{\mathrm{SC}}\quad,\quad R_{s0}=-\left.\frac{dV}{dI}\right|_{\mathrm{OC}} \tag{33}$$

As suggested in [54], for estimating the maximum power point MPP, first the P–V curve is computed with $P_i=I_i\cdot V_i$. Then, the measured discrete point with the greatest value $P_z=I_z\cdot V_z$ is considered and all the experimental points $(V_i,\ P_i)$ verifying $P_i\geq 85\%\cdot P_z$ are selected for a fifth-degree polynomial interpolation.

Next step is the derivation of the polynomial and the estimation of its real root inside the selected $X - range$. As a result, we can obtain a very good approximation of $P_{\max}$, V_{Pmax} and I_{Pmax}.

Before analysing the results of the parameter identification methods, the effect of the additional series resistances on the experimental I–V is shown in Figure 4. The plotted I–V curves are at the same irradiance and temperature conditions. In the figure it is evident how the increase of the series resistance affects significantly the knee of the I-V curves where is located the maximum power point and the slope in right part of the I-V curves.

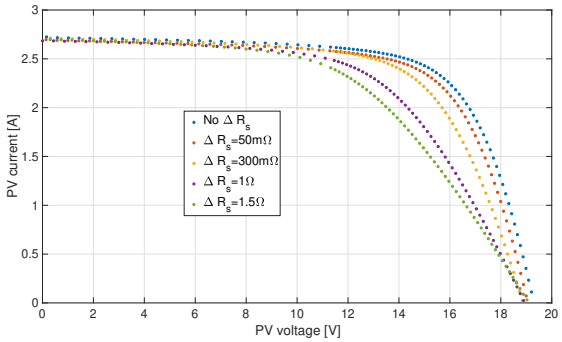

Figure 4: Experimental curves of PV panel under study with different added series resistances

4. Comparison of the identification methods in nominal conditions

The starting point for the comparative analysis of the methods is to estimate the five parameters at fixed conditions of in–plane irradiance and module temperature. From the pre-processed dataset of measured I–V curves, only those with cell temperature around a fixed value have been selected (a range of [43,44] °C has been chosen in order to maximise the number of measurements).

The set of I–V curves is then identified with $\{C[i]\}_{i=1}^{r}$ and their respective measurements of irradiance and module temperature are $\{G_{\mathrm{I}}[i]\}_{i=1}^{r}$ and $\{T[i]\}_{i=1}^{r}$ respectively, r is the number of selected curves. Over each curve $C[i]$ it is possible to run all the proposed methods (let $m \in$ {Fitting, Phang, SPRatio, Toledo, LambertW}) by providing the five values vector:

$$\{I_{ph}[i], I_0[i], n[i], R_s[i], R_{sh}[i]\}^{(m)} \qquad i \in [1, ..., r] \tag{34}$$

The restricted range of temperature allows to make negligible the dependency of SDM parameters on temperature since it is almost constant. Differently, the measured irradiance range has a wide variation because it only fulfils the criterion $G_{\mathrm{I}} \geq 700$ Wm^{-2}, thus a linear regression analysis is applied on the calculated SDM values in order to account the dependency of parameters with respect to in-plane irradiance G_{I}. The regression analysis is performed for all the explicit methods shown in Section 2. The results of the fitting method is considered as reference.

For all the methods, the dark saturation current I_0 and diode ideality factor n do not exhibit significant dependency on the irradiance, since the *coefficient of determination*, usually denoted with R^2, is very low. In general, a high R^2 value indicates that the regression model fits with the experimental data. In [55], it is stated that a value of R^2 lower than 0.25 means that between the studied variables there is a very low or no correlation.

The parameters I_0 and n are considered not dependent on the irradiance G_{I} because this condition occurs in both cases.

For the other three parameters (I_{ph}, R_s and R_{sh}), the *coefficient of determination* and the corresponding equations of regression lines are reported in Figures 5 and 6. The figures also show the SDM parameter values calculated with each method by using the selected I–V experimental curves. The regression lines have been expressed as function of the standard irradiance condition $\mathrm{G_{STC}} = 1000\ \mathrm{Wm^{-2}}$ as follows:

$$\begin{aligned} I_{ph} &= \delta_{I_{ph}}^{(m)}(G_{\mathrm{I}} - \mathrm{G_{STC}}) + I_{ph\ \mathrm{STC}}^{(m)} \\ R_s &= \delta_{R_s}^{(m)}(G_{\mathrm{I}} - \mathrm{G_{STC}}) + R_{s\ \mathrm{STC}}^{(m)} \\ R_{sh} &= \delta_{R_{sh}}^{(m)}(G_{\mathrm{I}} - \mathrm{G_{STC}}) + R_{sh\ \mathrm{STC}}^{(m)} \end{aligned} \tag{35}$$

where, for a specific method m, $\delta_{I_{ph}}^{(m)}$, $\delta_{R_s}^{(m)}$ and $\delta_{R_{sh}}^{(m)}$ are the angular coefficient of the regression lines and $I_{ph\ \mathrm{STC}}^{(m)}$, $R_{s\ \mathrm{STC}}^{(m)}$ and $R_{sh\ \mathrm{STC}}^{(m)}$ are the offsets of these lines at $G_{\mathrm{I}} = \mathrm{G_{STC}}$

By referring to the Figure 5, it is evident that the estimated I_{ph} values are strongly dependent on G_{I} since R^2 is almost equal to 1 for each method. This is an expected result because the photo-generated current depends linearly on the irradiance reaching the PV panel surface.

The regression lines of Figure 6 show that the series and parallel resistance dependency on the irradiance is also affected by the applied identification method. Indeed, by considering the results of the fitting method as reference, the other methods exhibit different angular coefficients and offsets. In some cases, the coefficient of determination R^2 is too low, meaning a non-dependency on G_{I}.

In addition to the regression analysis, the comparison of the calculated values by the explicit methods with respect to the results of the fitting method put into evidence that *Phang* method gives better results in R_s identification, while *LambertW* method is more effective in the R_{sh} identification. It is also evident that for the *SPRatio* method the identified R_s is always zero because $SPR < 1$.

Table 4 collects the average values $\mu(\cdot)$ and the standard deviation $\sigma(\cdot)$ of all SDM parameters calculated with the explicit methods and the fitting one.

Results show that each method converges towards different SDM parameters solutions, especially for the dark saturation current I_0. This issue has been already discussed in [56], where it has been shown that very dissimilar sets of the SDM parameters lead to either identical or very close I-V characteristics. For this reason, once the five parameters have been estimated for any experimental curve, the *MAPE* (Mean Absolute Percentage Error) of the main electrical parameters (I_{SC} , V_{OC}, P_{max}, I_{Pmax} and V_{Pmax}) is estimated by the following equation:

$$MAPE = \frac{100}{r} \cdot \sum_{i=1}^{r} \left| \frac{y_i - \tilde{y_i}}{y_i} \right| \tag{36}$$

where y_i is the value of I_{SC} , V_{OC}, P_{max}, I_{Pmax} or V_{Pmax} calculated directly from the experimental curve and $\tilde{y_i}$ is the same electrical parameter extracted by the I–V curve calculated with the single diode model by using the five parameters estimated by each explicit and fitting methods.

A Global Curve Error (*GCE*) based on the similarity between experimental and analytical I-V curves is also computed. The GCE takes into account the error in all the *current-voltage* pairs in the first quadrant of the I-V plane, it is calculated by considering the area enclosed between the two curves. The relative percentage curve error (*GCE [%]*) is obtained dividing the global error by the area below the experimental curve. As described

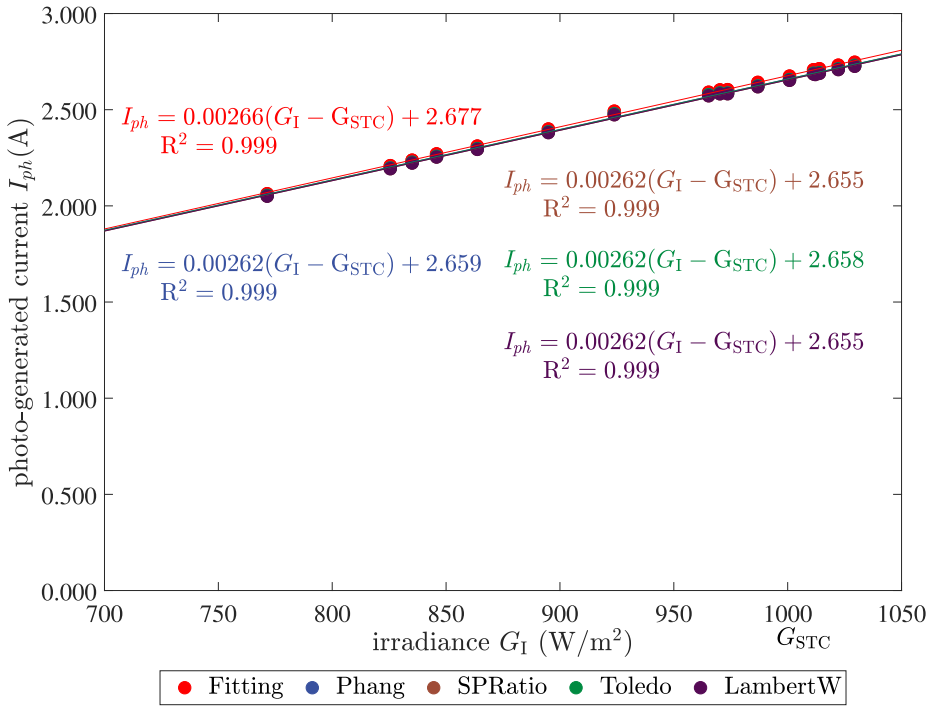

Figure 5: I_{ph} estimation at different irradiance conditions with respective regression lines

in [57], this procedure is not depending on the distribution of the experimental points along the curve and the numerical result is more precise. The *MAPE* errors as well as the relative curve error for each method are shown in Table 5.

It is noticeable that all the explicit methods, except *LambertW*, have approximated the short-circuit current I_{SC} with much more accuracy than the fitting method. This can be easily justified by the fact that the fitting method performs a global optimisation while explicit methods are working by using only notable points and slopes. For the open-circuit voltage all of them achieves similar results, being *LambertW* the less accurate. The case is the same when predicting the maximum power, but for this case, *Phang* method is slightly worse than the other ones. It is very interesting the behaviour of *SPRatio* to estimate the exact location of the MPP, because it not only achieves a very precise maximum power estimation, but also is almost as good as the fitting procedure for obtaining the pair (V_{Pmax},I_{Pmax}). When analysing the global curve error (similarity between curves), Fitting, Phang and Toledo get very good results.

5. Results with additional series resistance

Once the ability of the different methods to estimate the values of the parameters at nominal conditions has been tested, the next step is to study their behaviour when additional resistance is connected in series to the module terminals. Specifically, we want to compare the capacity of the different methods to detect correctly the emulated variation of the PV series resistance. In other words, when a series resistance of a nominal value ρ is added, a particular method m estimates a value of serial resistance equal to $R_s^{(m)}(\rho)$ that is expected to account the emulated variation. The objective would be to calculate how much greater is this value with respect to $R_s^{(m)}(0\ \Omega)$ that is the value without additional resistance, then $\Delta R_s^{(m)}(\rho) = R_s^{(m)}(\rho) - R_s^{(m)}(0\ \Omega)$ is

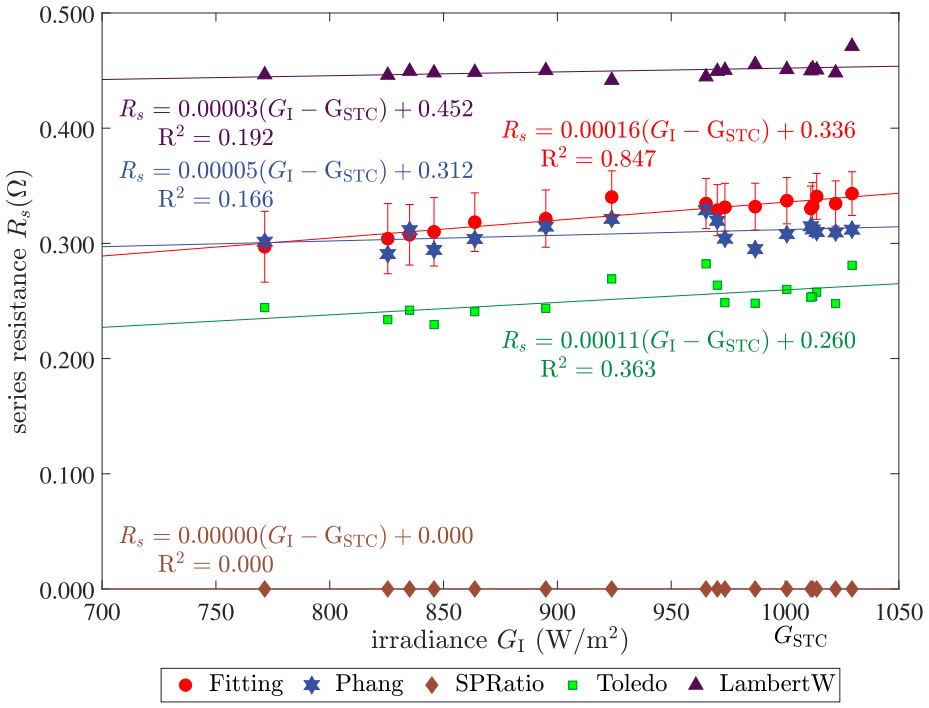

(a) R_s estimation with respective regression lines

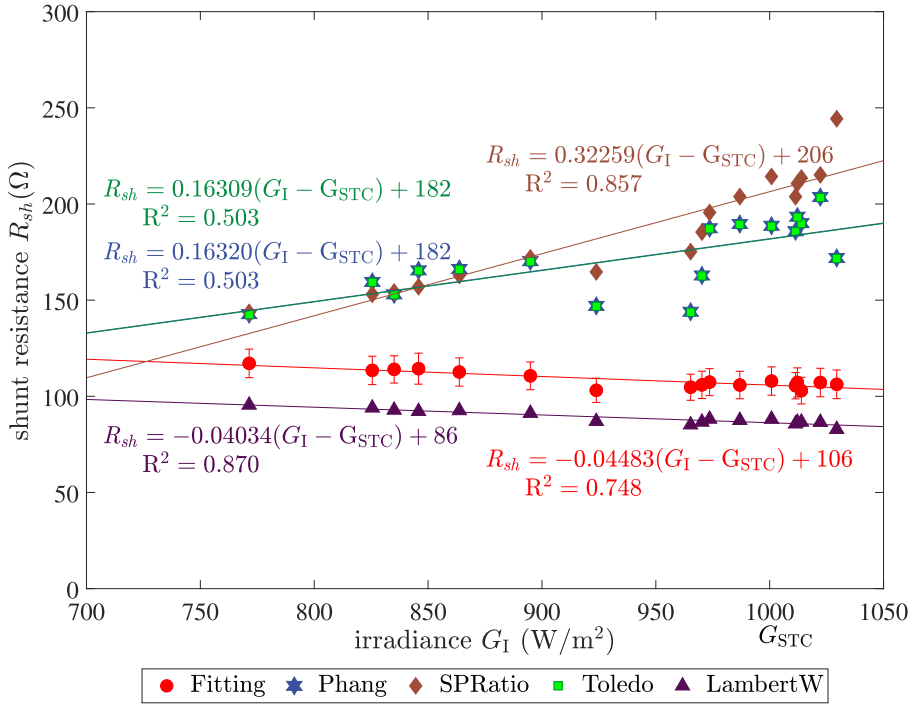

(b) R_{sh} estimation with respective regression lines

Figure 6: Estimations of series and parallel resistances at different irradiance conditions by using the selected identification methods

the estimation of ρ provided by the method m.

In order to compare the R_s estimation belonging to different experiments ($\rho = 0\ \Omega$, $\rho = 0.3\ \Omega$, $\rho = 1\ \Omega$, $\rho = 1.5\ \Omega$), they should be referred to the same level of irradiance G_I. However, each experiment has been

Table 4: Mean value μ and standard deviation σ of the 5 SDM calculated by different methods

		Fitting	Phang	SPRatio	Toledo	LambertW
$\mu(I_{ph})$	[A]	2.677	2.659	2.655	2.658	2.655
$\sigma(I_{ph})$	[A]	0.006	0.006	0.006	0.007	0.006
$\mu(I_0)$	[μA]	0.52	1.8	25	3.0	0.0079
$\sigma(I_0)$	[μA]	0.11	0.7	13	1.0	0.0007
$\mu(n)$		1.282	1.39	1.69	1.44	1.004
$\sigma(n)$		0.010	0.03	0.07	0.03	0.002
$\mu(R_s)$	[Ω]	0.336	0.312	0.000	0.260	0.452
$\sigma(R_s)$	[Ω]	0.005	0.009	0.000	0.012	0.005
$\mu(R_{sh})$	[Ω]	105.8	182	206	182	86.3
$\sigma(R_{sh})$	[Ω]	2.1	13	10	13	1.3

Table 5: *MAPE* of electrical parameters and global curve error *(GCE)*

		LambertW	Phang	SPRatio	Toledo	Fitting
I_{SC}	[%]	0.5	0.0003	0.0015	0.00010	0.4
V_{OC}	[%]	0.4	0.13	0.11	0.11	0.14
P_{max}	[%]	0.10	0.15	0.08	0.11	0.08
I_{Pmax}	[%]	0.6	0.9	0.3	0.6	0.3
V_{Pmax}	[%]	0.7	0.7	0.3	0.5	0.21
GCE	[%]	1.4	0.3	0.9	0.3	0.3

performed under outdoor conditions on different days, being the sequence of the values of incident irradiance G_{I} different from one experiment to other. Therefore, it is very difficult to find two estimations of R_s from different experiments but with the same irradiance. This issue has been solved by using the regression lines of R_s estimated in the previous experiments (eq 35) without PV degradation. Indeed, for each method the corresponding regression line allows to estimate the value of R_s for a given irradiance G_{I} when $\rho = 0\ \Omega$. In this way, for each experimental *I-V* curve measured with an additional series resistance ρ and under an irradiance $G_{\mathrm{I}}[i]$, the $R_s^{(m)}(\rho)[i]$ is estimated directly with the method m whereas the value $R_s^{(m)}(0\ \Omega)[i]$ in $G_{\mathrm{I}}[i]$ is calculated by using the regression line.

The regression lines are then calculated for the points $\{G_{\mathrm{I}}[i], \Delta R_s^{(m)}(\rho)[i]\}$, to study if there is any correlation between the detected resistance variation $\Delta R_s^{(m)}$ and the incident irradiance G_{I}. The values $\Delta R_s^{(m)}(\rho)$ should be as close as possible to the added resistance ρ and independent on the irradiance (the regression line should be flat and R^2 very close to zero).

The results of these calculations for the different methods can be seen in Figure 7 and Figure 8. In every figure, six lines have been plotted but three of them are common: the regression lines of $\Delta R_s^{(F)}(0.3\ \Omega)$, $\Delta R_s^{(F)}(1.0\ \Omega)$ and $\Delta R_s^{(F)}(1.5\ \Omega)$ where $^{(F)}$ stands for the *Fitting method* that is still representing the reference. The other three lines of each figure correspond to $\Delta R_s^{(m)}(0.3\ \Omega)$, $\Delta R_s^{(m)}(1.0\ \Omega)$ and $\Delta R_s^{(m)}(1.5\ \Omega)$, being

$m \in \{Phang,\ Toledo,\ LambertW,\ SPRatio\}$ in the different figures.

By comparing the four explicit methods with respect to the fitting results it is shown that *Phang* and *Toledo* methods are very effective in the identification of ΔR_s. *LambertW* method gives always an underestimation of ΔR_s. Moreover, the higher the added resistance the higher the error $\Delta R_s - \rho$, hence *LambertW* method is not suitable to identify the SDM parameters for a highly degraded PV panel. As concerns the *SPRatio*, the assumption that R_s is neglected when the coefficient $SPR < 1$ says that the method is not able to detect degradation when the PV series resistance is low. Nevertheless, *SPR* is itself a potential discrete indicator of degradation because when the series resistance increases the *SPR* indicators becomes higher than 1 indicating that the R_s cannot be neglected.

Table 6: Mean value μ and standard deviation σ of the parameters with additional $R_s = 1.5\ \Omega$

		Fitting	Phang	SPRatio	Toledo	LambertW
$\mu(I_{ph})$	[A]	2.688	2.659	2.624	2.659	2.624
$\sigma(I_{ph})$	[A]	0.004	0.004	0.003	0.004	0.003
$\mu(I_0)$	[μA]	0.34	0.92	57	1.2	0.0086
$\sigma(I_0)$	[μA]	0.03	0.07	5	0.1	0.0004
$\mu(n)$		1.240	1.323	1.829	1.347	1.0027
$\sigma(n)$		0.01	0.02	0.01	0.02	0.002
$\mu(R_s)$	[Ω]	1.858	1.831	1.532	1.809	1.722
$\sigma(R_s)$	[Ω]	0.003	0.003	0.004	0.003	0.002
$\mu(R_{sh})$	[Ω]	89.4	137	∞	135	58.4
$\sigma(R_{sh})$	[Ω]	1.2	4		4	0.4

Table 6 shows the identified SDM parameters while Table 7 reports the *MAPE* of the main electrical parameters and global curve error for the experimental cases performed with the additional series resistance $\rho = 1.5\ \Omega$. Again *LambertW* does not give satisfying results in terms of global curve error. Focusing on the others explicit methods, is confirmed that although they do not provide a set of identified parameters close to the results obtained by the *Fitting Method*, they are able to reproduce the *I–V* curves with a global curve error very small, providing a good similarity between experimental and analytical *I–V* curves. Indeed, the *I–V* curves shown in Figure 9 are almost overlapped with experimental results except for the *LambertW* method that provides an *I-V* plot slightly different. This happens in both normal and degraded conditions by confirming that such comparison is not enough to verify which methods is more effective to estimate correctly the R_s variation and, as a consequence, to detect the PV degradation properly.

6. Conclusions

An experimental validation of explicit methods used for the SDM parameter identification has been carried out in this paper. The analysis has been focused on the series resistance identification in presence of degraded *I-V* curves. Among them *Phang* method exhibits good capability to estimate both the R_s resistance as well as the emulated additional series resistance ΔR_s.

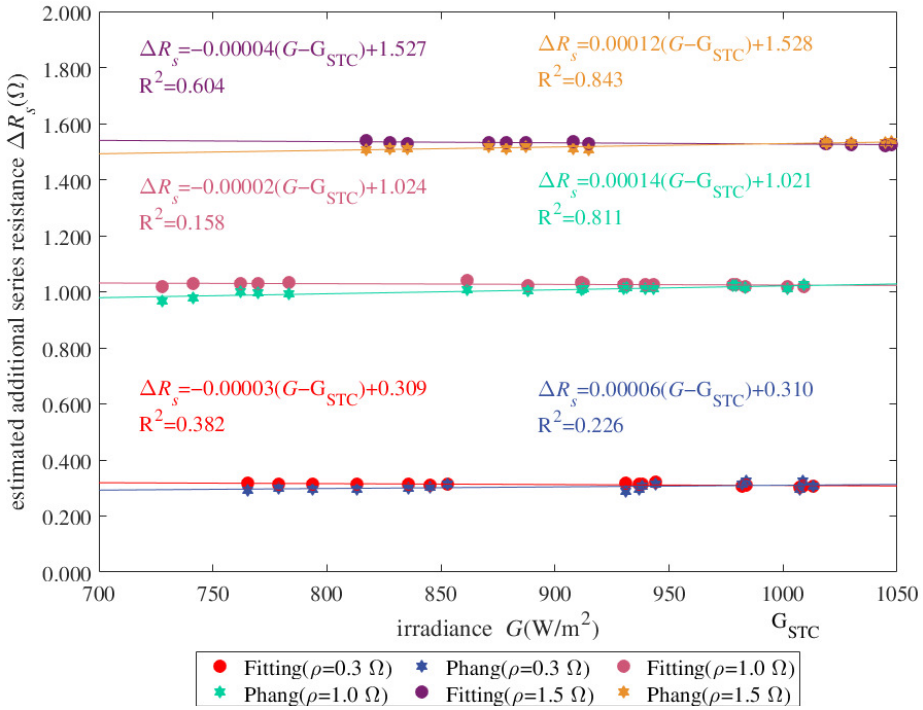

(a) Phang vs. Fitting

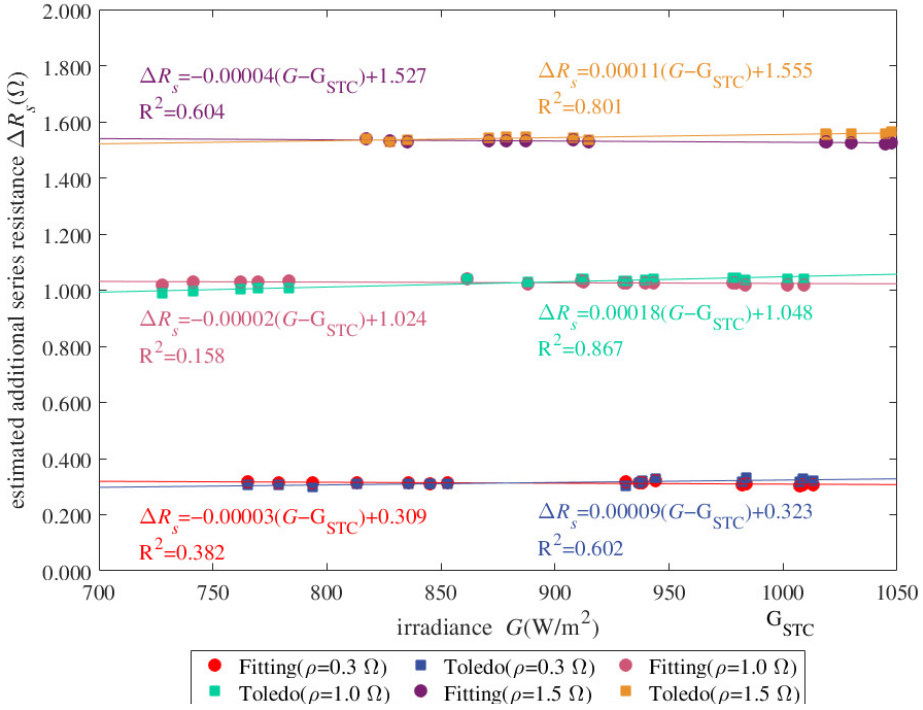

(b) Toledo vs. Fitting

Figure 7: Detection of additional series resistance ΔR_s for Phang and Toledo methods

Toledo method gives an underestimation in the R_s calculation but it is strongly accurate in ΔR_s estimation because the error of R_s calculated in nominal is almost totally compensated by the error of R_s calculated in degraded condition.

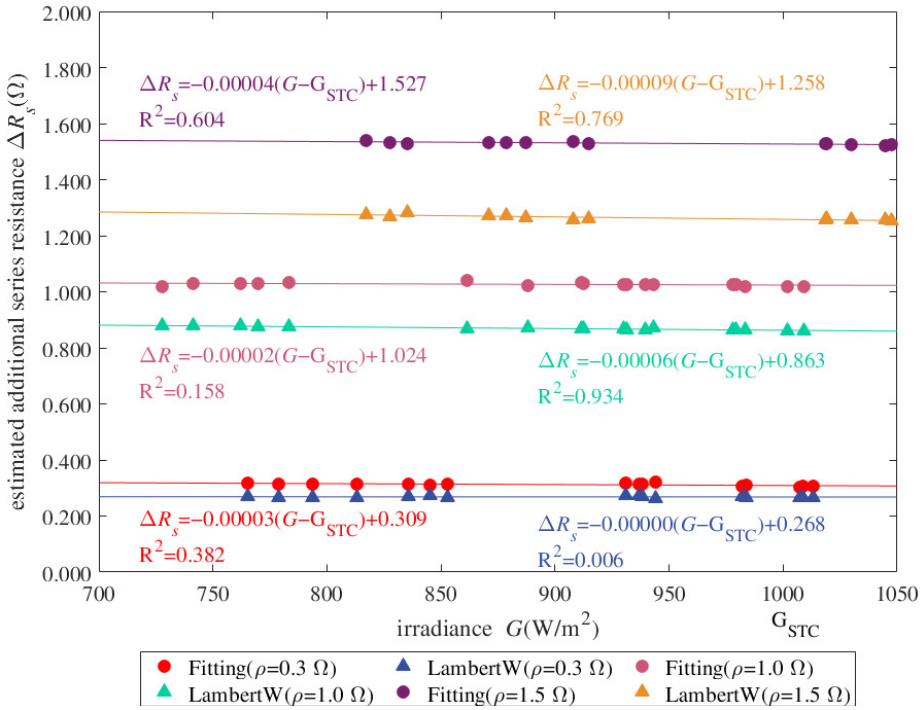

(a) LambertW vs. Fitting

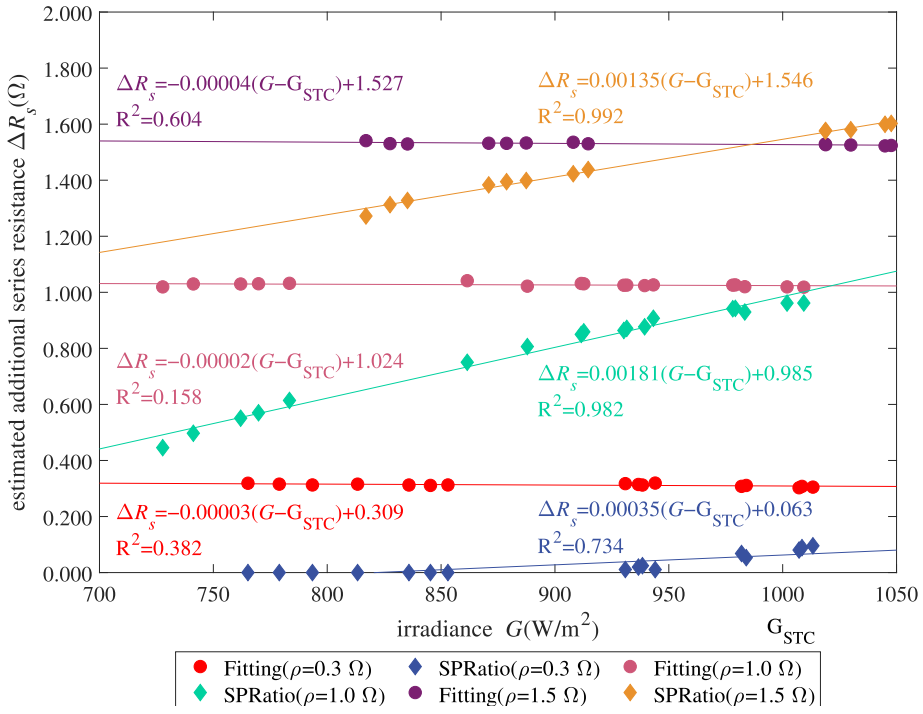

(b) SPRatio vs. Fitting

Figure 8: Detection of additional series resistance ΔR_s for LambertW and SPRatio methods

LambertW method is less accurate in R_s calculation and moreover the ΔR_s estimation worsens as the additional series resistance increases. This method seems more effective in the evaluation of R_{sh} parameter.

SPRatio method gives bad results in R_s and ΔR_s calculation, nevertheless the SPR coefficient could be used

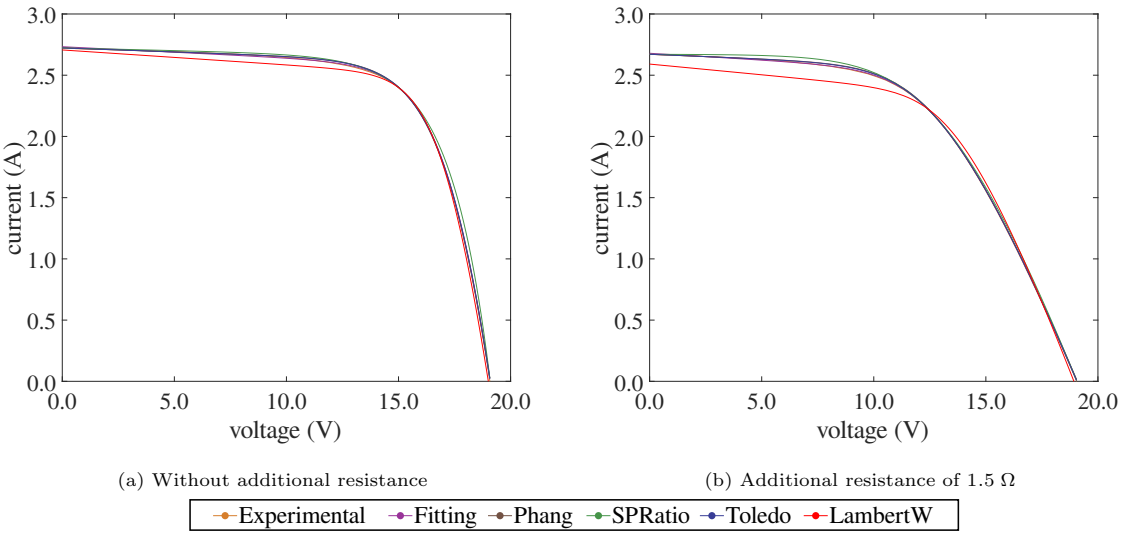

(a) Without additional resistance

(b) Additional resistance of 1.5 Ω

Figure 9: Comparison between experimental and simulated curves for different experiments

Table 7: *MAPE* of electrical parameters and global curve error (*GCE*) with $\Delta R_s = 1.5\,\Omega$

		LambertW	Phang	SPRatio	Toledo	Fitting
I_{SC}	[%]	3	0.004	0.007	0.0014	0.3
V_{OC}	[%]	0.6	0.22	0.12	0.11	0.15
P_{max}	[%]	0.6	0.3	0.12	0.12	0.10
I_{Pmax}	[%]	3	0.6	0.015	0.4	0.11
V_{Pmax}	[%]	4	0.3	0.10	0.24	0.09
GCE	[%]	4	0.4	1.2	0.3	0.20

as discrete indicator for degradation since it strongly depends on the R_s variation. *SPRatio* method gives also and almost exact location of the MPP point both in nominal and degraded conditions.

The analysis reported in this paper, although is not exhaustive, allows to assess that some set of explicit equations provide accurate evaluation of PV series resistance therefore suitable to be implemented on embedded systems for online parameters identification. Further analysis are currently ongoing by testing other explicit methods by using also different *I–V* curves databases in order to generalise the provided results.

ACKNOWLEDGMENTS

This work has been supported by MIUR funds in the frame of *PRIN 2017-Holistic approach to EneRgy-efficient smart nanOGRIDS (HEROGRIDS)* project (*2017WA5ZT3_003*), and by FARB funds of the University of Salerno. In addition, some resources are due to the project RTI2018–095097–B–I00 of the Ministerio de Ciencia, Innovación y Universidades, Spain.

References

[1] J.-W. Arnulf, Pv status report 2019, Publications Office of the European Uniondoi:10.2760/326629.
URL https://publications.jrc.ec.europa.eu/repository/bitstream/JRC118058/kjna29938enn_

1.pdf

[2] H. Dag, M. Buker, Performance evaluation and degradation assessment of crystalline silicon based photovoltaic rooftop technologies under outdoor conditions, Renewable Energy 156 (2020) 1292 – 1300. doi:https://doi.org/10.1016/j.renene.2019.11.141.
URL http://www.sciencedirect.com/science/article/pii/S096014811931835X

[3] E. L. Meyer, E. E. van Dyk, Assessing the reliability and degradation of photovoltaic module performance parameters, IEEE Transactions on Reliability 53 (1) (2004) 83–92. doi:10.1109/TR.2004.824831.

[4] P. Sánchez-Friera, M. Piliougine, J. Peláez, J. Carretero, M. Sidrach de Cardona, Analysis of degradation mechanisms of crystalline silicon PV modules after 12 years of operation in Southern Europe, Progress in Photovoltaics: Research and Applications 19 (6) (2011) 658–666. doi:10.1002/pip.1083.

[5] S. R. Madeti, S. Singh, Monitoring system for photovoltaic plants: A review, Renewable and Sustainable Energy Reviews 67 (2017) 1180 – 1207. doi:https://doi.org/10.1016/j.rser.2016.09.088.
URL http://www.sciencedirect.com/science/article/pii/S1364032116305792

[6] J. D. Bastidas-Rodriguez, G. Petrone, C. A. Ramos-Paja, G. Spagnuolo, Photovoltaic modules diagnostic: An overview, in: IECON 2013 - 39th Annual Conference of the IEEE Industrial Electronics Society, 2013, pp. 96–101. doi:10.1109/IECON.2013.6699117.

[7] F. D. Lia, S. Castello, L. Abenante, Efficiency degradation of c-silicon photovoltaic modules after 22-year continuous field exposure, in: 3rd World Conference onPhotovoltaic Energy Conversion, 2003. Proceedings of, Vol. 2, 11-1, pp. 2105–2108 Vol.2, ISBN: 4-9901816-0-3.

[8] J. A. Kratochvil, W. E. Boyson, D. L. King, Photovoltaic array performance model., Tech. rep., Sandia National Laboratories, Albuquerque (NM, USA), SAND2004-3535 (2004). doi:10.2172/919131.

[9] A. Kimber, T. Dierauf, L. Mitchell, C. Whitaker, T. Townsend, J. NewMiller, D. King, J. Granata, K. Emery, C. Osterwald, D. Myers, B. Marion, A. Pligavko, A. Panchula, T. Levitsky, J. Forbess, F. Talmud, Improved test method to verify the power rating of a photovoltaic (PV) project, in: 34th IEEE Photovoltaic Specialists Conference (PVSC), 2009, pp. 000316–000321. doi:10.1109/PVSC.2009.5411670.

[10] A. Cuevas, R. A. Sinton, Characterisation and diagnosis of silicon wafers and devices, Elsevier Science, Oxford (UK), 2005, Ch. IIb-4, pp. 163 – 188, ISBN: 978-1-85617-457-2. doi:10.1016/B978-185617457-2/50008-1.

[11] M. Piliougine, C. Cañete, R. Moreno, J. Carretero, J. Hirose, S. Ogawa, M. Sidrach de Cardona, Comparative analysis of energy produced by photovoltaic modules with anti-soiling coated surface in arid climates, Applied Energy 112 (2013) 626 – 634. doi:10.1016/j.apenergy.2013.01.048.

[12] A. Phinikarides, N. Kindyni, G. Makrides, G. E. Georghiou, Review of photovoltaic degradation rate methodologies, Renewable and Sustainable Energy Reviews 40 (2014) 143 – 152. doi:10.1016/j.rser.2014.07.155.

[13] D. L. King, W. Boyson, B. Hansen, W. Bower, Improved accuracy for low-cost solar irradiance sensors, in: 2nd World Conference and Exhibition on Photovoltaic Solar Energy Conversion, 1998. doi:10.2172/661542.

[14] A. Kumar, S. Gomathinayagam, G. Giridhar, I. Mitra, R. Vashistha, R. Meyer, M. Schwandt, K. Chhatbar, Field experiences with the operation of solar radiation resource assessment stations in India, Energy Procedia 49 (2014) 2351 – 2361. doi:10.1016/j.egypro.2014.03.249.

[15] Y. Li, K. Ding, J. Zhang, F. Chen, X. Chen, J. Wu, A fault diagnosis method for photovoltaic arrays based on fault parameters identification, Renewable Energy 143 (2019) 52–63. doi:https://doi.org/10.1016/j.renene.2019.04.147.
URL https://www.sciencedirect.com/science/article/pii/S0960148119306317

[16] E. L. Meyer, Extraction of saturation current and ideality factor from measuring V_{OC} and I_{SC} of photovoltaic modules, International Journal of Photoenergy 2017 (2017) 9. doi:10.1155/2017/8479487.

[17] N. Femia, G. Petrone, G. Spagnuolo, M. Vitelli, Power Electronics and Control Techniques for Maximum Energy Harvesting in Photovoltaic Systems, CRC Press, 2013, ISBN: 978-1-4665-0690-9.

[18] N. Aoun, N. Bailek, Evaluation of mathematical methods to characterize the electrical parameters of photovoltaic modules, Energy Conversion and Management 193 (2019) 25 – 38. doi:10.1016/j.enconman.2019.04.057.

[19] K. Ishaque, Z. Salam, S. Mekhilef, A. Shamsudin, Parameter extraction of solar photovoltaic modules using penalty-based differential evolution, Applied Energy 99 (2012) 297 – 308. doi:10.1016/j.apenergy.2012.05.017.

[20] F. J. Toledo, J. M. Blanes, Analytical and quasi-explicit four arbitrary point method for extraction of solar cell single-diode model parameters, Renewable Energy 92 (2016) 346–356. doi:10.1016/j.renene.2016.02.012.

[21] D. Kler, Y. Goswami, K. Rana, V. Kumar, A novel approach to parameter estimation of photovoltaic systems using hybridized optimizer, Energy Conversion and Management 187 (2019) 486 – 511. doi:10.1016/j.enconman.2019.01.102.

[22] U. Eicker, Chapter 5 – Grid–connected photovoltaic systems, in: Solar Technologies for Buildings, John Wiley & Sons, Ltd, 2003, Ch. 5, pp. 201–242.
URL http://dx.doi.org/10.1002/0470868341.ch5

[23] E. Saloux, A. Teyssedou, M. Sorin, Explicit model of photovoltaic panels to determine voltages and currents at the maximum power point, Solar Energy 85 (5) (2011) 713 – 722. doi:10.1016/j.solener.2010.12.022.

[24] J. Cubas, S. Pindado, C. De Manuel, Explicit expressions for solar panel equivalent circuit parameters based on analytical formulation and the Lambert W-Function, Energies 7 (7) (2014) 4098–4115. doi:10.3390/en7074098.

[25] D. Sera, R. Teodorescu, Robust series resistance estimation for diagnostics of photovoltaic modules, in: 2009 35th Annual Conference of IEEE Industrial Electronics, 2009, pp. 800–805. doi:10.1109/IECON.2009.5415022.

[26] F. Ghani, G. Rosengarten, M. Duke, J. Carson, The numerical calculation of single-diode solar-cell modelling parameters, Renewable Energy 72 (2014) 105 – 112. doi:10.1016/j.renene.2014.06.035.

[27] E. van Dyk, E. Meyer, Analysis of the effect of parasitic resistances on the performance of photovoltaic modules, Renewable Energy 29 (3) (2004) 333 – 344. doi:10.1016/S0960-1481(03)00250-7.

[28] E. Batzelis, Non-iterative methods for the extraction of the single-diode model parameters of photovoltaic modules: A review and comparative assessment, Energies 12 (3). doi:10.3390/en12030358.

[29] L. Liu, W. Liu, X. Zhang, J. Ingenhoff, Research on the novel explicit model for photovoltaic i-v characteristic of the single diode model under different splitting spectrum, Results in Physics 12 (2019) 662 – 672. doi:10.1016/j.rinp.2018.12.021.

[30] J. C. H. Phang, D. S. H. Chan, J. R. Phillips, Accurate analytical method for the extraction of solar cell model parameters, Electronics Letters 20 (10) (1984) 406–408. doi:10.1049/el:19840281.

[31] L. Cristaldi, M. Faifer, M. Rossi, S. Toscani, A simplified model of photovoltaic panel, in: 2012 IEEE International Instrumentation and Measurement Technology Conference Proceedings, 2012, pp. 431–436. doi:10.1109/I2MTC.2012.6229672.

[32] D. Sera, L. Mathe, T. Kerekes, R. Teodorescu, P. Rodriguez, A low-disturbance diagnostic function integrated in the PV arrays'MPPT algorithm, in: IECON 2011 - 37th Annual Conference of the IEEE Industrial Electronics Society, 2011, pp. 2456–2460. doi:10.1109/IECON.2011.6119695.

[33] F. J. Toledo, J. M. Blanes, A. Garrigós, J. A. Martínez, Analytical resolution of the electrical four-parameters model of a photovoltaic module using small perturbation around the operating point, Renewable Energy 43 (2012) 83 – 89. doi:10.1016/j.renene.2011.11.037.

[34] F. J. Toledo, J. M. Blanes, Geometric properties of the single-diode photovoltaic model and a new very simple method for parameters extraction, Renewable Energy 72 (2014) 125–133. doi:10.1016/j.renene.2014.06.032.

[35] S. Cannizzaro, M. Di Piazza, M. Luna, G. Vitale, Generalized classification of PV modules by simplified single-diode models, in: Industrial Electronics (ISIE), 2014 IEEE 23rd International Symposium on, 2014, pp. 2266–2273. doi:10.1109/ISIE.2014.6864971.

[36] S. Cannizzaro, M. C. Di Piazza, M. Luna, G. Vitale, PVID: An interactive Matlab application for parameter identification of complete and simplified single-diode PV models, in: 2014 IEEE 15th Workshop on Control and Modeling for Power Electronics (COMPEL), 2014, pp. 1–7. doi:10.1109/COMPEL.2014.6877152.

[37] E. I. Batzelis, S. A. Papathanassiou, A method for the analytical extraction of the single-diode PV model parameters, IEEE Transactions on Sustainable Energy 7 (2) (2016) 504–512. doi:10.1109/TSTE.2015.2503435.

[38] A. Senturk, R. Eke, A new method to simulate photovoltaic performance of crystalline silicon photovoltaic modules based on datasheet values, Renewable Energy 103 (2017) 58 – 69. doi:10.1016/j.renene.2016.11.025.

[39] NIST, 2018 CODATA recommended values of the fundamental constants of physics and chemistry SP 959. national institute of standard and technology. u.s. department of commerce (June 2019).
URL https://physics.nist.gov/cuu/pdf/wallet_2018.pdf

[40] M. Oulcaid, H. E. Fadil], L. Ammeh, A. Yahya, F. Giri, Parameter extraction of photovoltaic cell and module: Analysis and discussion of various combinations and test cases, Sustainable Energy Technologies and Assessments 40 (2020) 100736. doi:https://doi.org/10.1016/j.seta.2020.100736.
URL http://www.sciencedirect.com/science/article/pii/S2213138819308896

[41] V. J. Chin, Z. Salam, K. Ishaque, Cell modelling and model parameters estimation techniques for photovoltaic simulator application: A review, Applied Energy 154 (2015) 500 – 519. doi:https://doi.org/10.1016/j.apenergy.2015.05.035.
URL http://www.sciencedirect.com/science/article/pii/S0306261915006455

[42] G. Petrone, C. A. Ramos-Paja, G. Spagnuolo, Photovoltaic Sources Modeling, John Wiley & Sons, Chichester, West Sussex, United Kingdom, 2017, ISBN: 978-1-118-75612-6.

[43] R. M. Corless, G. H. Gonnet, D. E. G. Hare, D. J. Jeffrey, D. E. Knuth, On the lambertw function, Advances in Computational Mathematics 5 (1) (1996) 329–359. doi:10.1007/BF02124750.

[44] C. A. Ramos-Paja, G. Petrone, G. Spagnuolo, Symbolic algebra for the calculation of the series and parallel resistances in PV module model, in: International Conference on Clean Electrical Power Renewable Energy Resources Impact (ICCEP), Alghero, Sardinia, Italy, 2013, pp. 62–66, ISBN: 978-1-4673-4430-2.

[45] F. Lasnier, T. G. Ang, Photovoltaic Engineering Handbook, IOP Publishing, 1990, ISBN: 0-85274-311-4.

[46] A. R. Conn, N. I. M. Gould, P. L. Toint, Trust-Region Methods, SIAM Society for Industrial and Applied Mathematics, 2000, ISBN: 0-89871-460-5.

[47] T. Khatib, W. Elmenreich, Modeling of photovoltaic systems using Matlab, John Wiley & Sons, Hoboken, New Jersey (USA), 2016, ISBN: 978-1-119-11810-7.

[48] B. R. Zaharatos, M. Campanelli, L. Tenorio, On the estimability of the PV single-diode model parameters, Statistical Analysis and Data Mining: The ASA Data Science Journal 8 (5-6) (2015) 329–339. doi:10.1002/sam.11286.

[49] Matlab Optimization Toolbox. User's Guide. R2019b, MathWorks, Natick, Massachusetts (USA), 2019.
URL www.mathworks.com/help/pdf_doc/optim/optim_tb.pdf

[50] M. Piliougine, J. Carretero, L. Mora-López, M. Sidrach de Cardona, Experimental system for current–voltage curve measurement of photovoltaic modules under outdoor conditions, Progress in Photovoltaics: Research and Applications 19 (5) (2011) 591–602. doi:10.1002/pip.1073.

[51] M. Piliougine, J. Carretero, L. Mora-López, M. Sidrach de Cardona, New software tool to characterize photovoltaic modules from commercial equipment, WEENTECH Proceedings in Energy (2018) 211 – 220. doi:10.32438/WPE.6218.

[52] S. Kaplanis, E. Kaplani, Energy performance and degradation over 20 years performance of BP c–Si PV modules, Simulation Modelling Practice and Theory 19 (4) (2011) 1201 – 1211. doi:https://doi.org/10.1016/j.simpat.2010.07.009.
URL http://www.sciencedirect.com/science/article/pii/S1569190X10001711

[53] Z. Salam, K. Ishaque, H. Taheri, An improved two-diode photovoltaic (PV) model for PV system, in: 2010 Joint International Conference on Power Electronics, Drives and Energy Systems 2010 Power, India, 2010, pp. 1–5. doi:10.1109/PEDES.2010.5712374.

[54] K. Emery, Photovoltaic calibrations at the National Renewable Energy Laboratory and uncertainty analysis following the ISO 17025 guidelines, Tech. rep., National Renewable Energy Laboratory (NREL), Golden (CO, USA), NREL/TP-5J00-66873 (2016).
URL https://www.nrel.gov/docs/fy17osti/66873.pdf

[55] K. G. Calkins, Applied Statistics - Lesson 5 - Correlation Coefficients., Last visited: 14/07/2020 (July 2005).
URL www.andrews.edu/~calkins/math/edrm611/edrm05.htm

[56] M. B. Rhouma, A. Gastli, L. Ben Brahim, F. Touati, M. Benammar, A simple method for extracting the parameters of the pv cell single-diode model, Renewable Energy 113 (2017) 885 – 894. doi:https://doi.org/10.1016/j.renene.2017.06.064.
URL http://www.sciencedirect.com/science/article/pii/S0960148117305694

[57] M. Piliougine, D. Elizondo, L. Mora-López, M. Sidrach de Cardona, Modelling photovoltaic modules with neural networks using angle of incidence and clearness index, Progress in Photovoltaics: Research and Applications 23 (4) (2015) 513–523. doi:10.1002/pip.2449.